Higher-order Corrections to Quantum Observables in Semileptonic Higgs Decays

Alberto Navarro
Seoultech

Pheno 2026
May12, 2026

Based on arXiv.2604.16218 with D. Gonçalves and A. Kaladharan

Introduction

- Higgs decays to Z and W bosons is one of the most prominent channels to probe quantum information phenomena between two qutrits and new physics at colliders.
- Very recent results on spin correlations from both ATLAS and CMS for the 4 charged lepton final state.

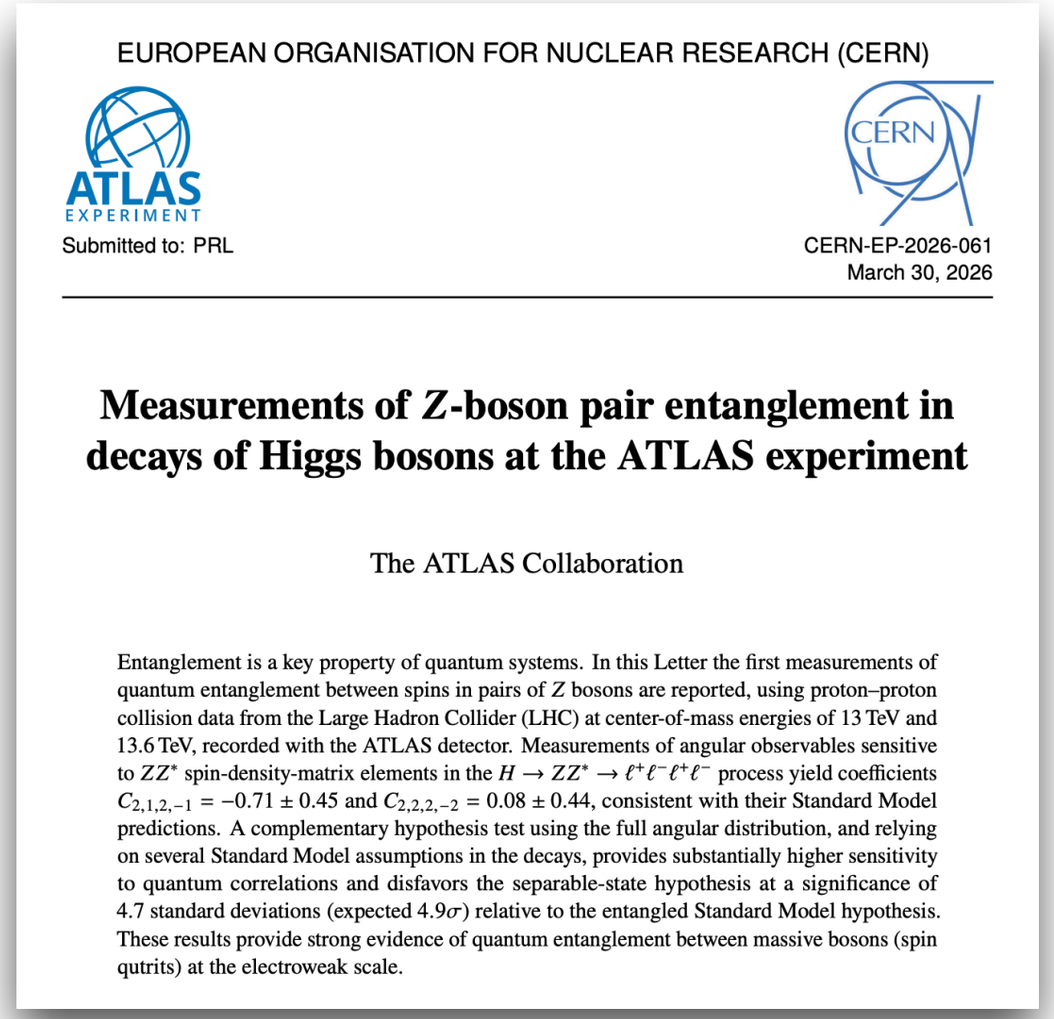

EUROPEAN ORGANISATION FOR NUCLEAR RESEARCH (CERN)

ATLAS EXPERIMENT

CERN

Submitted to: PRL

CERN-EP-2026-061
March 30, 2026

Measurements of Z-boson pair entanglement in decays of Higgs bosons at the ATLAS experiment

The ATLAS Collaboration

Entanglement is a key property of quantum systems. In this Letter the first measurements of quantum entanglement between spins in pairs of Z bosons are reported, using proton–proton collision data from the Large Hadron Collider (LHC) at center-of-mass energies of 13 TeV and 13.6 TeV, recorded with the ATLAS detector. Measurements of angular observables sensitive to ZZ^* spin-density-matrix elements in the $H \to ZZ^* \to \ell^+\ell^-\ell^+\ell^-$ process yield coefficients $C_{2,1,2,-1} = -0.71 \pm 0.45$ and $C_{2,2,2,-2} = 0.08 \pm 0.44$, consistent with their Standard Model predictions. A complementary hypothesis test using the full angular distribution, and relying on several Standard Model assumptions in the decays, provides substantially higher sensitivity to quantum correlations and disfavors the separable-state hypothesis at a significance of 4.7 standard deviations (expected 4.9σ) relative to the entangled Standard Model hypothesis. These results provide strong evidence of quantum entanglement between massive bosons (spin qutrits) at the electroweak scale.

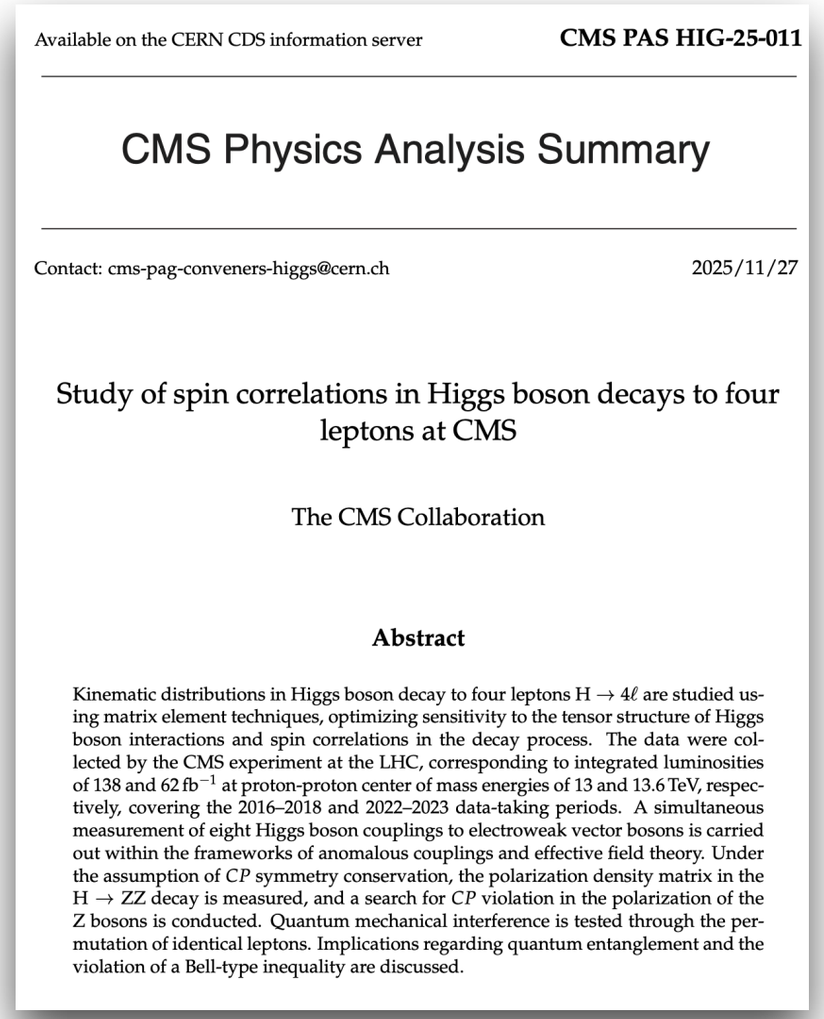

Available on the CERN CDS information server

CMS PAS HIG-25-011

CMS Physics Analysis Summary

Contact: cms-pag-conveners-higgs@cern.ch

2025/11/27

Study of spin correlations in Higgs boson decays to four leptons at CMS

The CMS Collaboration

Abstract

Kinematic distributions in Higgs boson decay to four leptons $H \to 4\ell$ are studied using matrix element techniques, optimizing sensitivity to the tensor structure of Higgs boson interactions and spin correlations in the decay process. The data were collected by the CMS experiment at the LHC, corresponding to integrated luminosities of 138 and 62 fb^{-1} at proton-proton center of mass energies of 13 and 13.6 TeV, respectively, covering the 2016–2018 and 2022–2023 data-taking periods. A simultaneous measurement of eight Higgs boson couplings to electroweak vector bosons is carried out within the frameworks of anomalous couplings and effective field theory. Under the assumption of CP symmetry conservation, the polarization density matrix in the $H \to ZZ$ decay is measured, and a search for CP violation in the polarization of the Z bosons is conducted. Quantum mechanical interference is tested through the permutation of identical leptons. Implications regarding quantum entanglement and the violation of a Bell-type inequality are discussed.

Talk by R. Demina this morning

- Possibility to extend the analysis to WW decays

Barr (2021)
Fabbri, Howarth, Maurin (2023)

Introduction

- Reconstruction of the spin density matrix from the angular correlations of the final-state products through a quantum tomography procedure.
- This procedure relies on some assumptions for the mapping from the angular correlations to the density matrix.

Grossi, Pelliccioli, Vicini (2024)
Del Grata, Fabbri, Lamba, Maltoni, Pagani (2025)
Gonçalves, Kaladharan, Krauss, Navarro (2025)
Aguilar-Saavedra (2025)
Gonçalves, Kaladharan, Navarro (2025)
Del Grata et al (2025)
Aguilar-Saavedra, Giardino (2026)

Also F. Maltoni's talk

- Studies of the effects of next-to-leading order EW corrections in h->4l show that the quantum tomography procedure is very sensitive to NLO effects.
- Effects are channel dependent with smaller effects for leptonic h->WW* than leptonic h->ZZ*. See Dorival's talk
- Assessing the stability of the quantum tomography is then crucial for proper characterization of the VV quantum state at colliders.
- Precise determination of the angular correlations also important for BSM searches.
- Extending such studies to semileptonic decays, which offer more statistics, is then relevant for future experimental analyses.

Quantum Tomography of the VV* System

- The quantum state of the VV system is represented by a 9x9 density matrix

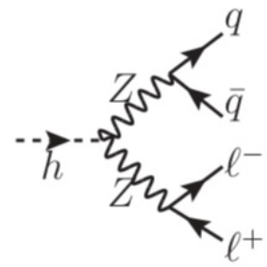

$$\rho = \frac{1}{9}\left(\mathbb{I}_3 \otimes \mathbb{I}_3 + A^1_{LM} T^L_M \otimes \mathbb{I}_3 + A^2_{LM} \mathbb{I}_3 \otimes T^L_M + C_{L_1 M_1 L_2 M_2} T^{L_1}_{M_1} \otimes T^{L_2}_{M_2}\right) .$$

- Full differential distribution for their production and decay

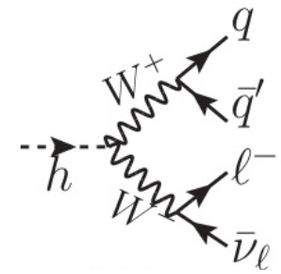

$$\frac{1}{\sigma}\frac{d\sigma}{d\Omega_1 d\Omega_2} = \frac{1}{(4\pi)^2}\left[1 + A^1_{LM} B_L Y^M_L(\theta_1,\varphi_1) + A^2_{LM} B_L Y^M_L(\theta_2,\varphi_2) + C_{L_1 M_1 L_2 M_2} B_{L_1} B_{L_2} Y^{M_1}_{L_1}(\theta_1,\varphi_1) Y^{M_2}_{L_2}(\theta_2,\varphi_2)\right] .$$

- Angular coefficients extracted from the differential distribution using orthogonality of the spherical harmonics

Aguilar-Saavedra, Bernal, Casas, Moreno (2023)

$$\frac{1}{\sigma}\int \frac{d\sigma}{d\Omega_1 d\Omega_2} Y^M_L(\Omega_i)^* d\Omega_1 d\Omega_2 = \frac{B_L}{4\pi} A^i_{LM},$$

$$\frac{1}{\sigma}\int \frac{d\sigma}{d\Omega_1 d\Omega_2} Y^{M_1}_{L_1}(\Omega_1)^* Y^{M_2}_{L_2}(\Omega_2)^* d\Omega_1 d\Omega_2 = \frac{B_{L_1} B_{L_2}}{(4\pi)^2} C_{L_1 M_1 L_2 M_2} .$$

$$B_1 = -\sqrt{2\pi}\,\eta_f$$

$$B_2 = \sqrt{2\pi/5}\,(1 - 3\delta_f)$$

- The constants B1 and B2 depend on the type of vector boson and final-state fermions through the spin analyzing power, η_f, and mass correction, δ_f.

Quantum Tomography of the VV* System

- The quantum state of the VV system is represented by a 9x9 density matrix

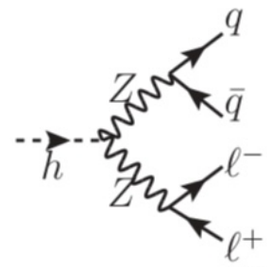

$$\rho = \frac{1}{9}\left(\mathbb{I}_3 \otimes \mathbb{I}_3 + A^1_{LM} T^L_M \otimes \mathbb{I}_3 + A^2_{LM} \mathbb{I}_3 \otimes T^L_M + C_{L_1 M_1 L_2 M_2} T^{L_1}_{M_1} \otimes T^{L_2}_{M_2}\right) .$$

- Full differential distribution for their production and decay

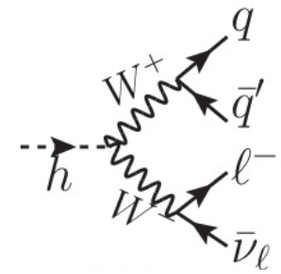

$$\frac{1}{\sigma}\frac{d\sigma}{d\Omega_1 d\Omega_2} = \frac{1}{(4\pi)^2}\left[1 + A^1_{LM} B_L Y^M_L(\theta_1,\varphi_1) + A^2_{LM} B_L Y^M_L(\theta_2,\varphi_2) + C_{L_1 M_1 L_2 M_2} B_{L_1} B_{L_2} Y^{M_1}_{L_1}(\theta_1,\varphi_1) Y^{M_2}_{L_2}(\theta_2,\varphi_2)\right] .$$

- Angular coefficients extracted from the differential distribution using orthogonality of the spherical harmonics

Aguilar-Saavedra, Bernal, Casas, Moreno (2023)

$$\frac{1}{\sigma}\int \frac{d\sigma}{d\Omega_1 d\Omega_2} Y^M_L(\Omega_i)^* d\Omega_1 d\Omega_2 = \frac{B_L}{4\pi} A^i_{LM},$$

$$\frac{1}{\sigma}\int \frac{d\sigma}{d\Omega_1 d\Omega_2} Y^{M_1}_{L_1}(\Omega_1)^* Y^{M_2}_{L_2}(\Omega_2)^* d\Omega_1 d\Omega_2 = \frac{B_{L_1} B_{L_2}}{(4\pi)^2} C_{L_1 M_1 L_2 M_2} .$$

$$B_1 = -\sqrt{2\pi}\,\eta_f$$

$$B_2 = \sqrt{2\pi/5}\,(1 - 3\delta_f)$$

- In the massless final-state fermions limit

$$\eta_f = \frac{C_L^2 - C_R^2}{C_L^2 + C_R^2} \qquad \delta_f = 0$$

Final-state Mass Effects

- First consider the final-state fermion masses effects on the angular moments

$$\frac{1}{\sigma}\int \frac{d\sigma}{d\Omega_1 d\Omega_2} Y_L^M(\Omega_i)^*\, d\Omega_1 d\Omega_2 \equiv f^i_{LM},$$

$$\frac{1}{\sigma}\int \frac{d\sigma}{d\Omega_1 d\Omega_2} Y_{L_1}^{M_1}(\Omega_1)^* Y_{L_2}^{M_2}(\Omega_2)^*\, d\Omega_1 d\Omega_2 \equiv g_{L_1 M_1 L_2 M_2}.$$

	$h \to \ell^+\ell^- b\bar{b}$			$h \to \ell^+\ell^- c\bar{c}$		
	$m_b = 0$	$m_b = 4.5$ GeV	Ratio	$m_c = 0$	$m_c = 1.3$ GeV	Ratio
Selections: $m_{\ell\ell} > 10$ GeV, $m_{q\bar{q}} > 10$ GeV						
$f^1_{2,0}$	$-0.04794(9)$	$-0.04839(9)$	$1.009(2)$	$-0.04801(9)$	$-0.04795(9)$	$0.998(3)$
$f^2_{2,0}$	$-0.04798(9)$	$-0.04093(9)$	$0.853(2)$	$-0.04785(9)$	$-0.04706(9)$	$0.983(3)$
$g_{1,0,1,0}$	$-0.00498(2)$	$-0.00471(2)$	$0.946(7)$	$-0.00367(2)$	$-0.00374(2)$	$1.019(8)$
$g_{1,1,1,-1}$	$0.00781(2)$	$0.00747(2)$	$0.956(3)$	$0.00582(2)$	$0.00585(2)$	$1.005(5)$
$g_{2,1,2,-1}$	$-0.00776(2)$	$-0.00703(2)$	$0.906(3)$	$-0.00775(2)$	$-0.00766(2)$	$0.988(3)$
$g_{2,0,2,0}$	$0.01094(2)$	$0.00978(2)$	$0.893(2)$	$0.01097(2)$	$0.01081(2)$	$0.985(3)$
$g_{2,2,2,-2}$	$0.00492(2)$	$0.00454(2)$	$0.922(5)$	$0.00487(2)$	$0.00484(2)$	$0.993(5)$
Selections: $m_{\ell\ell} > 20$ GeV, $\lvert m_{q\bar{q}} - m_Z\rvert < 10$ GeV						
$f^1_{2,0}$	$-0.02915(9)$	$-0.02936(9)$	$1.007(4)$	$-0.0294(1)$	$-0.0293(1)$	$0.997(4)$
$f^2_{2,0}$	$-0.02925(9)$	$-0.02911(9)$	$0.995(4)$	$-0.0292(1)$	$-0.0293(1)$	$1.003(4)$
$g_{1,0,1,0}$	$-0.00622(3)$	$-0.00609(3)$	$0.979(7)$	$-0.00454(3)$	$-0.00459(3)$	$1.011(9)$
$g_{1,1,1,-1}$	$0.00839(2)$	$0.00835(2)$	$0.995(3)$	$0.00622(2)$	$0.00622(2)$	$1.000(4)$
$g_{2,1,2,-1}$	$-0.00833(2)$	$-0.00819(2)$	$0.983(3)$	$-0.00828(2)$	$-0.00826(2)$	$0.997(3)$
$g_{2,0,2,0}$	$0.00977(2)$	$0.00964(3)$	$0.986(4)$	$0.00980(3)$	$0.00972(3)$	$0.991(4)$
$g_{2,2,2,-2}$	$0.00612(2)$	$0.00604(2)$	$0.987(4)$	$0.00607(2)$	$0.00607(2)$	$1.000(5)$

Gonçalves, Kaladharan, **AN** (2026)

Final-state Mass Effects

- First consider the final-state fermion masses effects on the angular moments

$$\frac{1}{\sigma}\int \frac{d\sigma}{d\Omega_1 d\Omega_2} Y_L^M(\Omega_i)^*\, d\Omega_1 d\Omega_2 = \frac{B_L}{4\pi} A^i_{LM} \equiv f^i_{LM},$$

$$\frac{1}{\sigma}\int \frac{d\sigma}{d\Omega_1 d\Omega_2} Y_{L_1}^{M_1}(\Omega_1)^* Y_{L_2}^{M_2}(\Omega_2)^*\, d\Omega_1 d\Omega_2 = \frac{B_{L_1} B_{L_2}}{(4\pi)^2} C_{L_1 M_1 L_2 M_2} \equiv g_{L_1 M_1 L_2 M_2}.$$

- In the Higgs decay to VV* at least one of the boson is off-shell. There is an extra scalar component for the propagator of the off-shell V*.

- Such component vanishes when coupled to massless final-state fermions so that the mapping from f and g to A and C is just a rescaling by B1 and B2. For massive final states, the mapping is not exact.

- Effects can be suppressed requiring the hadronic bosons to be close to its mass shell.

$$|m_{\mathrm{V_{had}}} - m_{\mathrm{V}}| < 10 \text{ GeV},\ m_{\ell\ell} > 20 \text{ GeV}$$

	$h \to \ell^+\nu_\ell \bar{c}s$			$h \to \ell^+\ell^- c\bar{c}$			$h \to \ell^+\ell^- b\bar{b}$		
	$m_c = 0$	$m_c = 1.3$ GeV	Ratio	$m_c = 0$	$m_c = 1.3$ GeV	Ratio	$m_b = 0$	$m_b = 4.5$ GeV	Ratio
$A^1_{2,0}$	$-0.564(1)$	$-0.560(1)$	$0.993(2)$	$-0.329(1)$	$-0.329(1)$	$1.000(4)$	$-0.327(1)$	$-0.329(1)$	$1.006(4)$
$A^2_{2,0}$	$-0.564(1)$	$-0.560(1)$	$0.993(2)$	$-0.328(1)$	$-0.329(1)$	$1.003(4)$	$-0.327(1)$	$-0.328(1)$	$1.003(4)$
$C_{1,0,1,0}$	$-0.6035(9)$	$-0.6062(9)$	$1.004(4)$	$-0.766(4)$	$-0.773(4)$	$1.009(7)$	$-0.774(3)$	$-0.764(3)$	$0.987(5)$
$C_{1,1,1,-1}$	$0.9560(9)$	$0.9555(9)$	$0.999(2)$	$1.047(4)$	$1.048(4)$	$1.001(5)$	$1.046(3)$	$1.046(3)$	$1.000(4)$
$C_{2,1,2,-1}$	$-0.952(3)$	$-0.956(3)$	$1.004(4)$	$-1.041(3)$	$-1.039(3)$	$0.998(4)$	$-1.046(3)$	$-1.035(3)$	$0.989(4)$
$C_{2,0,2,0}$	$1.396(4)$	$1.400(4)$	$1.003(4)$	$1.233(3)$	$1.223(3)$	$0.992(3)$	$1.228(4)$	$1.218(4)$	$0.991(4)$
$C_{2,2,2,-2}$	$0.607(4)$	$0.607(4)$	$1.000(9)$	$0.764(3)$	$0.764(3)$	$1.000(5)$	$0.770(3)$	$0.763(3)$	$0.991(5)$

Gonçalves, Kaladharan, **AN** (2026)

Entanglement in $h \to VV^*$ at LO

- Highly constrained density matrix due to symmetries of the decay

$$A_{20}^1 = A_{20}^2 \neq 0\,,$$
$$C_{1,1,1,-1} = C_{1,-1,1,1} = -C_{2,1,2,-1} = -C_{2,-1,2,1} \neq 0\,,$$
$$C_{2,2,2,-2} = C_{2,-2,2,2} = -C_{1,0,1,0} = 2 - C_{2,0,2,0} \neq 0\,,$$
$$\frac{A_{20}^{1,2}}{\sqrt{2}} + 1 = C_{2,2,2,-2}\,.$$

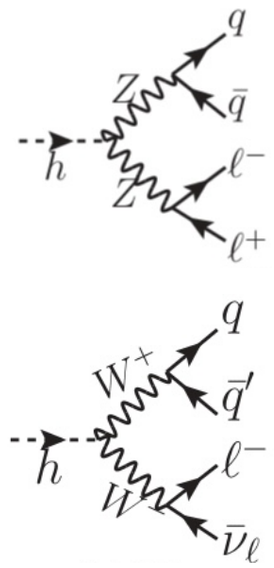

- Full density matrix parametrized by only two coefficients.

$$\rho_{\rm LO} = \begin{pmatrix}
0 & 0 & 0 & 0 & 0 & 0 & 0 & 0 & 0 \\
0 & 0 & 0 & 0 & 0 & 0 & 0 & 0 & 0 \\
0 & 0 & \frac{1}{3}C_{2,2,2,-2} & 0 & \frac{1}{3}C_{2,1,2,-1} & 0 & \frac{1}{3}C_{2,2,2,-2} & 0 & 0 \\
0 & 0 & 0 & 0 & 0 & 0 & 0 & 0 & 0 \\
0 & 0 & \frac{1}{3}C_{2,1,2,-1} & 0 & \frac{1}{3}\left(3 - 2C_{2,2,2,-2}\right) & 0 & \frac{1}{3}C_{2,1,2,-1} & 0 & 0 \\
0 & 0 & 0 & 0 & 0 & 0 & 0 & 0 & 0 \\
0 & 0 & \frac{1}{3}C_{2,2,2,-2} & 0 & \frac{1}{3}C_{2,1,2,-1} & 0 & \frac{1}{3}C_{2,2,2,-2} & 0 & 0 \\
0 & 0 & 0 & 0 & 0 & 0 & 0 & 0 & 0 \\
0 & 0 & 0 & 0 & 0 & 0 & 0 & 0 & 0
\end{pmatrix}.$$

Aguilar-Saavedra, Bernal, Casas, Moreno (2023)
Fabbrichesi, Floreanini, Gabrielli, Marzola (2023)

Entanglement in $h \to VV^*$ at LO

- Use concurrence bounds for entanglement

$$(\mathcal{C}(\rho))^2 \geq 2\,\max\left\{0,\,\mathrm{Tr}\left[\rho^2\right] - \mathrm{Tr}\left[\rho_A^2\right],\,\mathrm{Tr}\left[\rho^2\right] - \mathrm{Tr}\left[\rho_B^2\right]\right\} \equiv \mathscr{C}^2_{\mathrm{LB}},$$
$$(\mathcal{C}(\rho))^2 \leq 2\,\min\left\{1 - \mathrm{Tr}\left[\rho_A^2\right],\,1 - \mathrm{Tr}\left[\rho_B^2\right]\right\} \equiv \mathscr{C}^2_{\mathrm{UB}}\,.$$

Mintert, Buchleitner (2007)
Zhang, et al (2008)

- System is entangled throughout full phase space

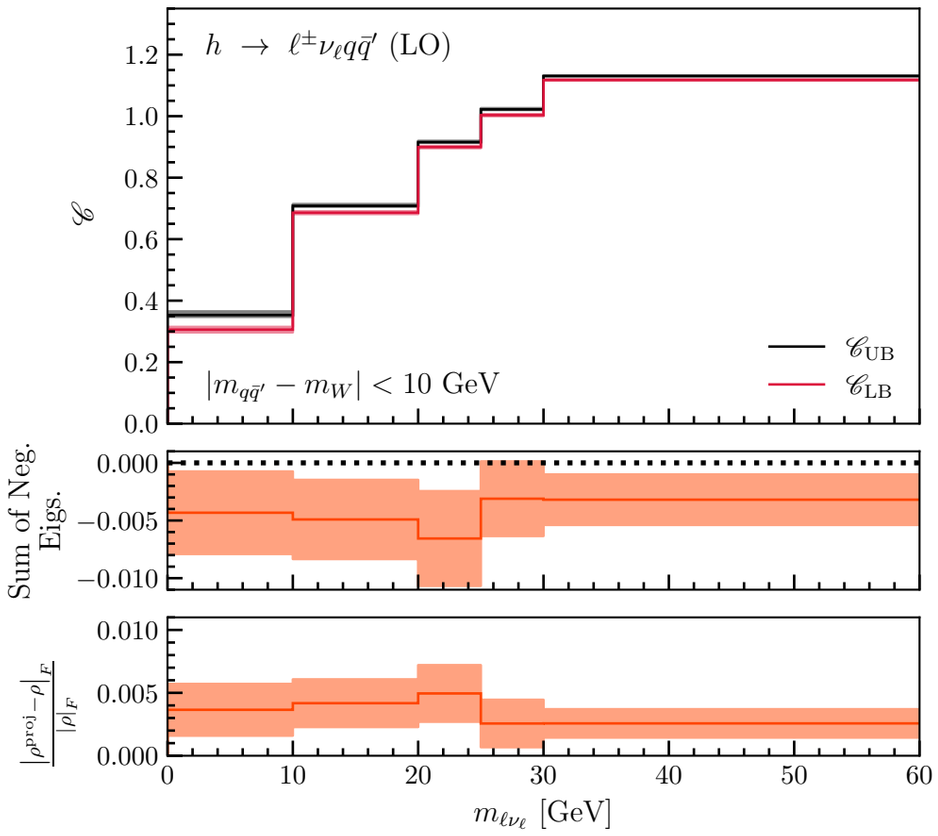

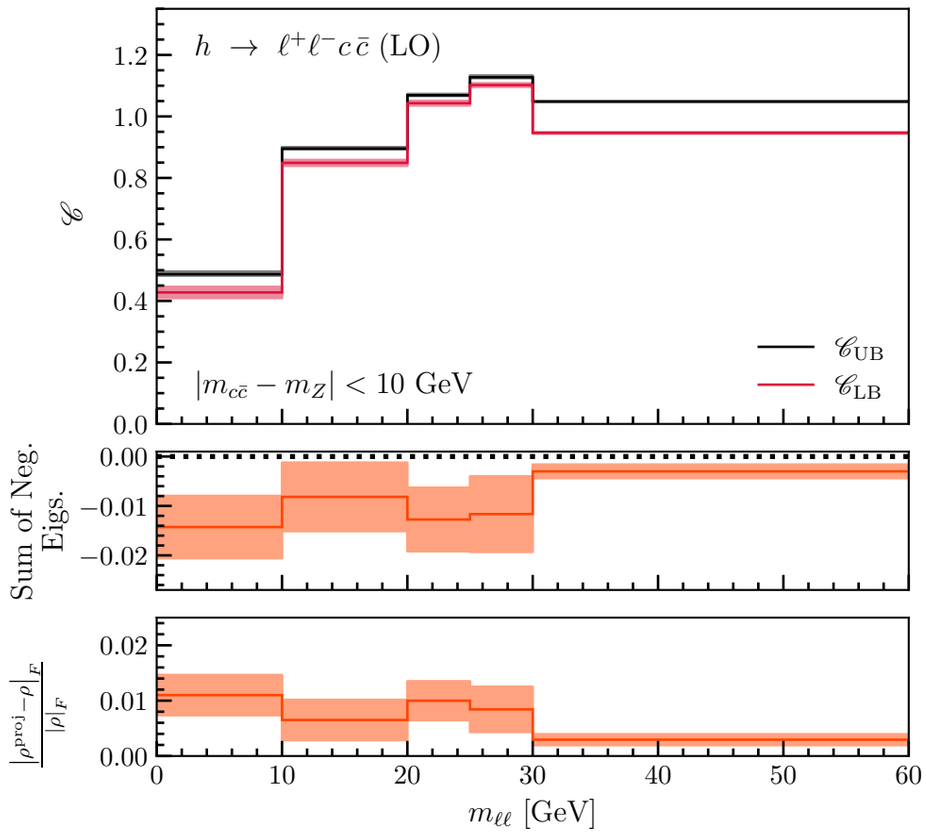

Gonçalves, Kaladharan, **AN** (2026)

$h \to VV^*$ at NLO QCD

- Effects only present for the hadronic side.
- New nonzero coefficients.
- Sensitivity to the choice of jet radius.

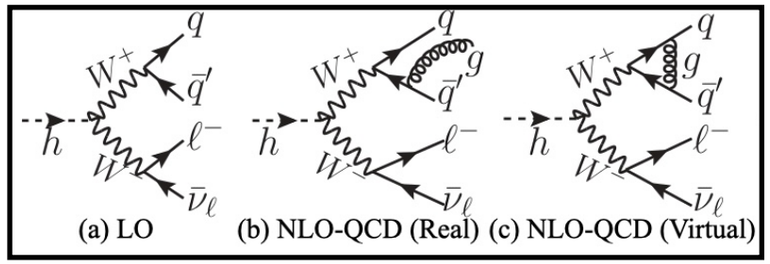

$h \to \ell^\pm \nu_\ell q \bar{q}'$					
	LO	$\text{NLO}_{R=0.4}$	$\text{NLO}_{R=0.4}/\text{LO}$	$\text{NLO}_{R=1}$	$\text{NLO}_{R=1}/\text{LO}$
$A^1_{2,0}$	$-0.564(1)$	$-0.5433(8)$	$0.963(2)$	$-0.556(4)$	$0.986(7)$
$A^2_{2,0}$	$-0.565(1)$	$-0.5411(8)$	$0.958(2)$	$-0.555(3)$	$0.982(6)$
$C_{1,1,1,-1}$	$0.9551(6)$	$0.946(4)$	$0.990(4)$	$0.948(2)$	$0.993(2)$
$C_{2,1,2,-1}$	$-0.952(2)$	$-0.95(2)$	$1.00(2)$	$-0.94(1)$	$1.00(1)$
$C_{1,0,1,0}$	$-0.6034(6)$	$-0.607(4)$	$1.006(7)$	$-0.602(2)$	$0.998(3)$
$C_{2,0,2,0}$	$1.399(3)$	$1.37(2)$	$0.98(1)$	$1.38(1)$	$0.986(7)$
$C_{2,2,2,-2}$	$0.603(3)$	$0.59(2)$	$0.98(3)$	$0.59(1)$	$0.98(2)$
$A^1_{2,1}$	0	$0.07(1)$	–	$0.054(7)$	–
$A^1_{2,2}$	0	$-0.08(1)$	–	$-0.066(8)$	–
$A^2_{2,1}$	0	$0.07(1)$	–	$0.055(7)$	–
$A^2_{2,2}$	0	$-0.08(1)$	–	$-0.066(8)$	–
$C_{1,1,1,1}$	0	$0.05(1)$	–	$0.037(5)$	–
$C_{1,1,1,0}$	0	$-0.026(6)$	–	$-0.020(3)$	–
$C_{1,0,1,1}$	0	$-0.025(6)$	–	$-0.019(3)$	–

Gonçalves, Kaladharan, **AN** (2026)

$h \to VV^*$ at NLO QCD

- Effects only present for the hadronic side.
- New nonzero coefficients.
- Sensitivity to the choice of jet radius.

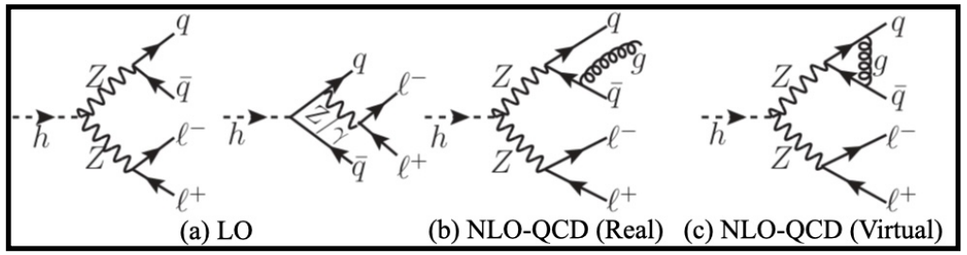

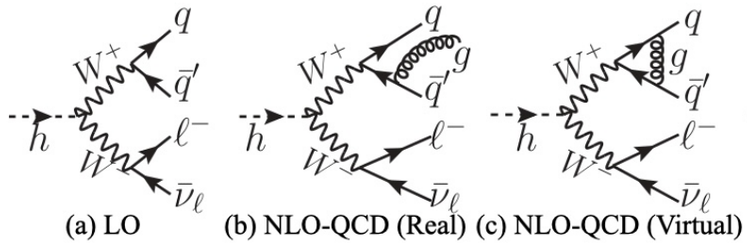

	$h \to \ell^+\ell^- c\bar{c}$				
	LO	$\text{NLO}_{R=0.4}$	$\text{NLO}_{R=0.4}/\text{LO}$	$\text{NLO}_{R=1}$	$\text{NLO}_{R=1}/\text{LO}$
$A^1_{2,0}$	$-0.329(1)$	$-0.316(8)$	$0.96(2)$	$-0.326(4)$	$0.99(1)$
$A^2_{2,0}$	$-0.328(1)$	$-0.29(1)$	$0.88(3)$	$-0.315(4)$	$0.96(2)$
$C_{1,1,1,-1}$	$1.047(4)$	$1.07(3)$	$1.02(3)$	$1.07(2)$	$1.02(2)$
$C_{2,1,2,-1}$	$-1.041(3)$	$-1.05(2)$	$1.01(2)$	$-1.04(1)$	$1.00(1)$
$C_{1,0,1,0}$	$-0.766(4)$	$-0.81(3)$	$1.06(4)$	$-0.79(1)$	$1.03(1)$
$C_{2,0,2,0}$	$1.233(3)$	$1.22(2)$	$0.99(2)$	$1.22(1)$	$0.989(8)$
$C_{2,2,2,-2}$	$0.764(3)$	$0.76(2)$	$0.99(2)$	$0.76(1)$	$0.99(1)$
$A^2_{2,1}$	0	$0.19(3)$	–	$0.14(2)$	–
$A^2_{2,2}$	0	$-0.21(3)$	–	$-0.16(2)$	–
$C_{2,0,2,2}$	0	$0.11(3)$	–	$0.08(2)$	–
	$h \to \ell^+\ell^- b\bar{b}$				
	LO	$\text{NLO}_{R=0.4}$	$\text{NLO}_{R=0.4}/\text{LO}$	$\text{NLO}_{R=1}$	$\text{NLO}_{R=1}/\text{LO}$
$A^1_{2,0}$	$-0.329(1)$	$-0.314(8)$	$0.95(2)$	$-0.321(5)$	$0.98(1)$
$A^2_{2,0}$	$-0.328(1)$	$-0.294(7)$	$0.90(2)$	$-0.313(4)$	$0.95(1)$
$C_{1,1,1,-1}$	$1.046(3)$	$1.04(2)$	$0.99(2)$	$1.03(2)$	$0.98(2)$
$C_{2,1,2,-1}$	$-1.035(3)$	$-1.05(3)$	$1.01(3)$	$-1.04(2)$	$1.00(2)$
$C_{1,0,1,0}$	$-0.764(3)$	$-0.80(2)$	$1.05(3)$	$-0.78(1)$	$1.02(1)$
$C_{2,0,2,0}$	$1.218(4)$	$1.22(2)$	$1.00(2)$	$1.22(1)$	$1.00(1)$
$C_{2,2,2,-2}$	$0.763(3)$	$0.77(2)$	$1.01(3)$	$0.76(2)$	$1.00(3)$
$A^2_{2,1}$	0	$0.06(1)$	–	$0.09(1)$	–
$A^2_{2,2}$	0	$-0.07(1)$	–	$-0.10(1)$	–
$C_{2,0,2,2}$	0	$0.03(2)$	–	$0.05(2)$	–

	$h \to \ell^\pm \nu_\ell q\bar{q}'$				
	LO	$\text{NLO}_{R=0.4}$	$\text{NLO}_{R=0.4}/\text{LO}$	$\text{NLO}_{R=1}$	$\text{NLO}_{R=1}/\text{LO}$
$A^1_{2,0}$	$-0.564(1)$	$-0.5433(8)$	$0.963(2)$	$-0.556(4)$	$0.986(7)$
$A^2_{2,0}$	$-0.565(1)$	$-0.5411(8)$	$0.958(2)$	$-0.555(3)$	$0.982(6)$
$C_{1,1,1,-1}$	$0.9551(6)$	$0.946(4)$	$0.990(4)$	$0.948(2)$	$0.993(2)$
$C_{2,1,2,-1}$	$-0.952(2)$	$-0.95(2)$	$1.00(2)$	$-0.94(1)$	$1.00(1)$
$C_{1,0,1,0}$	$-0.6034(6)$	$-0.607(4)$	$1.006(7)$	$-0.602(2)$	$0.998(3)$
$C_{2,0,2,0}$	$1.399(3)$	$1.37(2)$	$0.98(1)$	$1.38(1)$	$0.986(7)$
$C_{2,2,2,-2}$	$0.603(3)$	$0.59(2)$	$0.98(3)$	$0.59(1)$	$0.98(2)$
$A^1_{2,1}$	0	$0.07(1)$	–	$0.054(7)$	–
$A^1_{2,2}$	0	$-0.08(1)$	–	$-0.066(8)$	–
$A^2_{2,1}$	0	$0.07(1)$	–	$0.055(7)$	–
$A^2_{2,2}$	0	$-0.08(1)$	–	$-0.066(8)$	–
$C_{1,1,1,1}$	0	$0.05(1)$	–	$0.037(5)$	–
$C_{1,1,1,0}$	0	$-0.026(6)$	–	$-0.020(3)$	–
$C_{1,0,1,1}$	0	$-0.025(6)$	–	$-0.019(3)$	–

Gonçalves, Kaladharan, **AN** (2026)

$h \to VV^*$ at NLO QCD

- Overall milder effects on the reconstructed density matrix

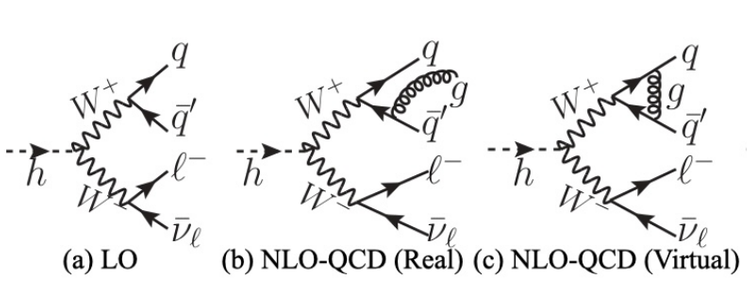

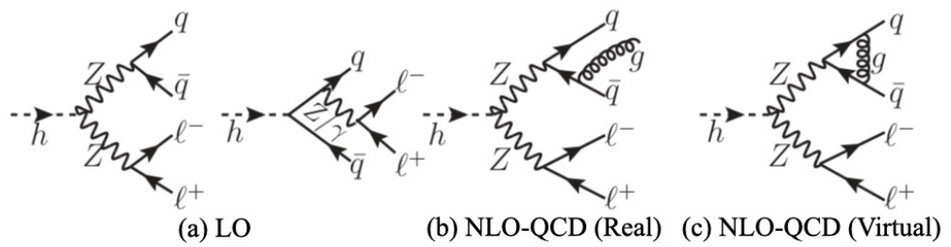

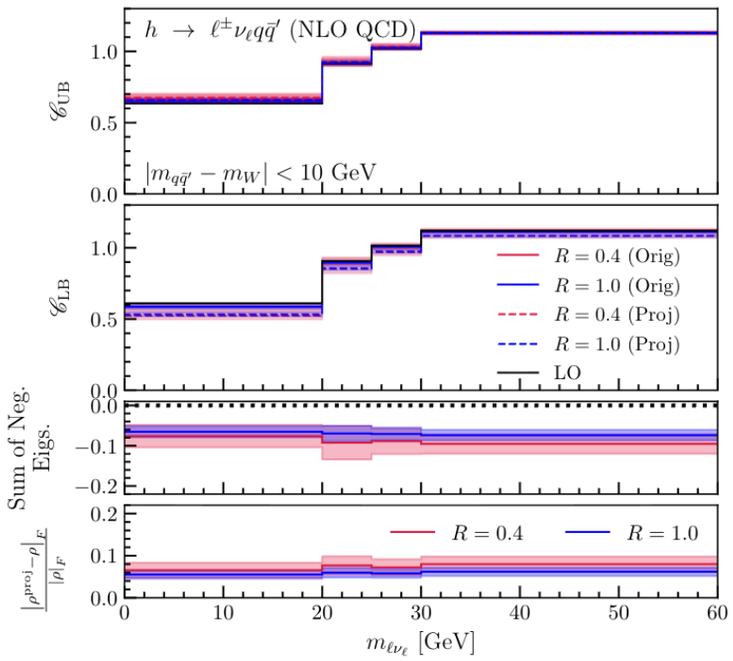

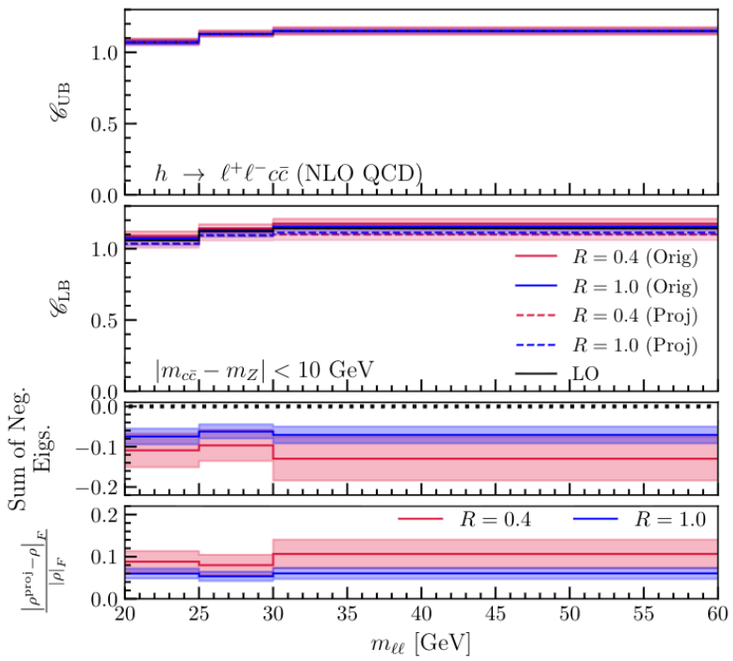

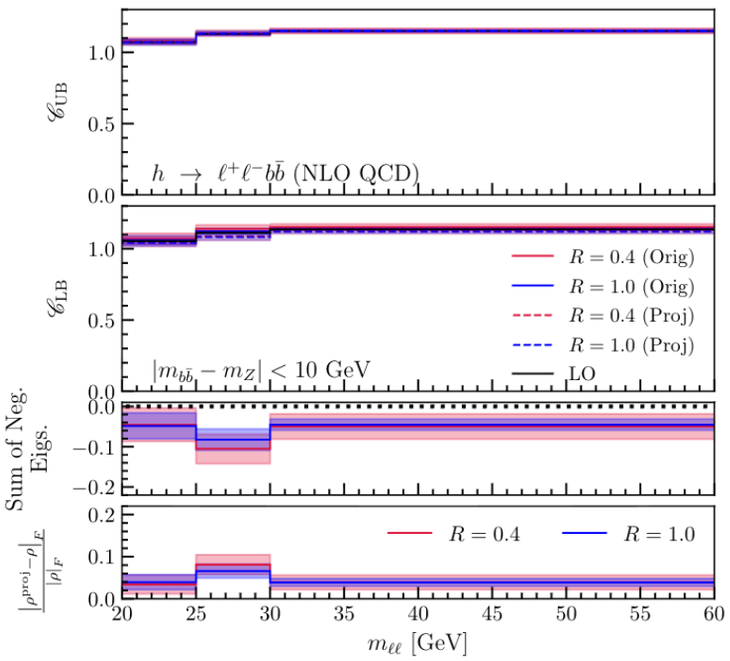

Gonçalves, Kaladharan, **AN** (2026)

$h \to VV^*$ at NLO QCD

- Overall milder effects on the reconstructed density matrix

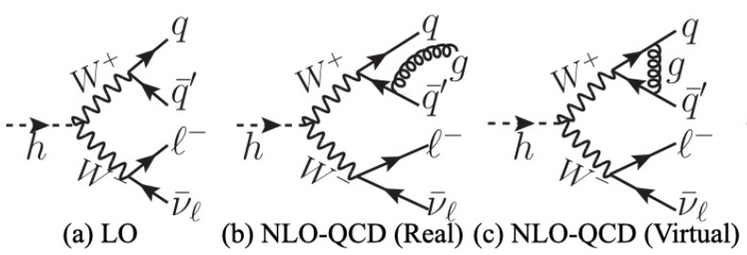

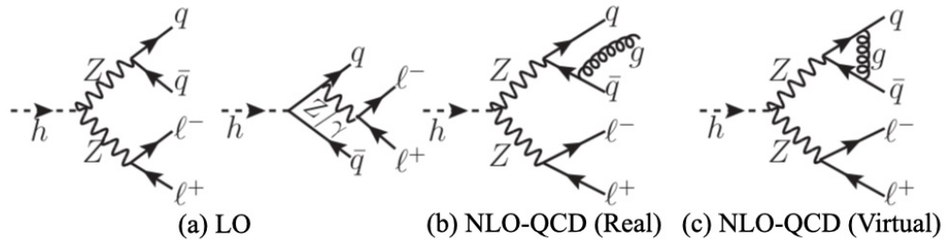

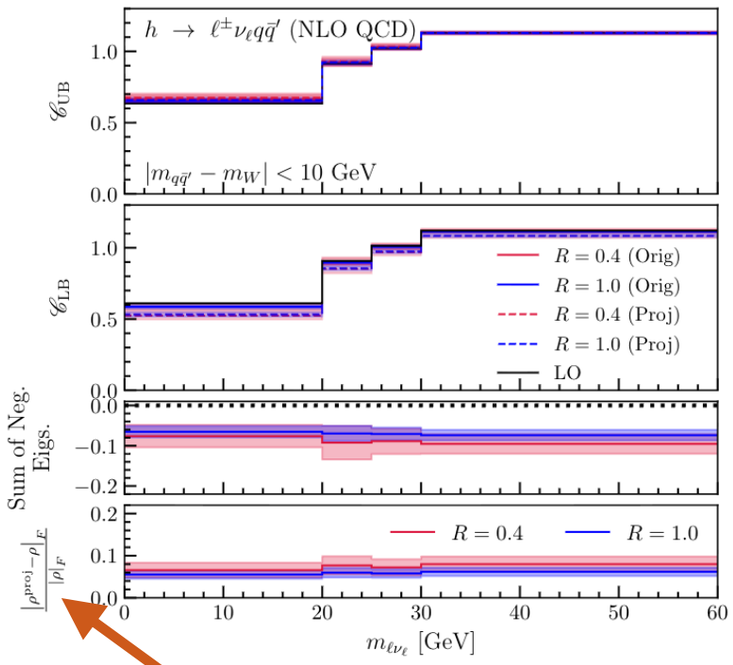

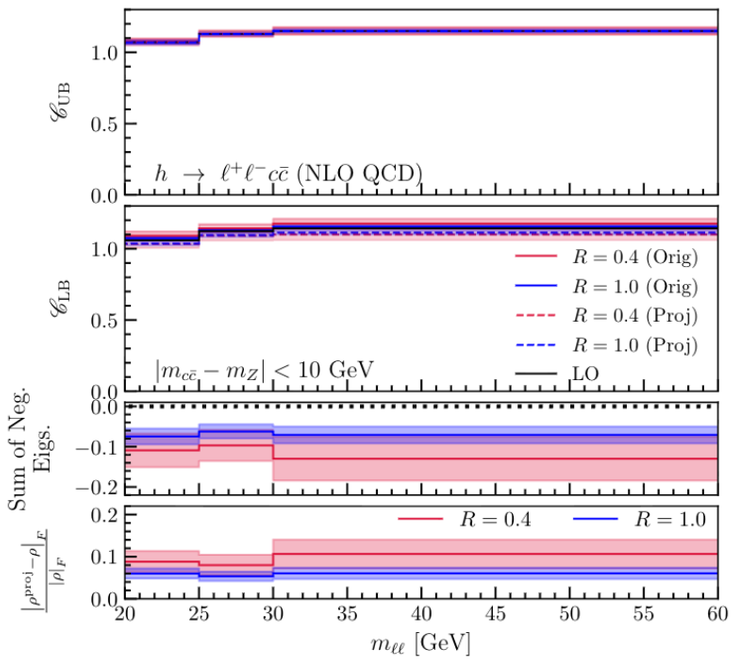

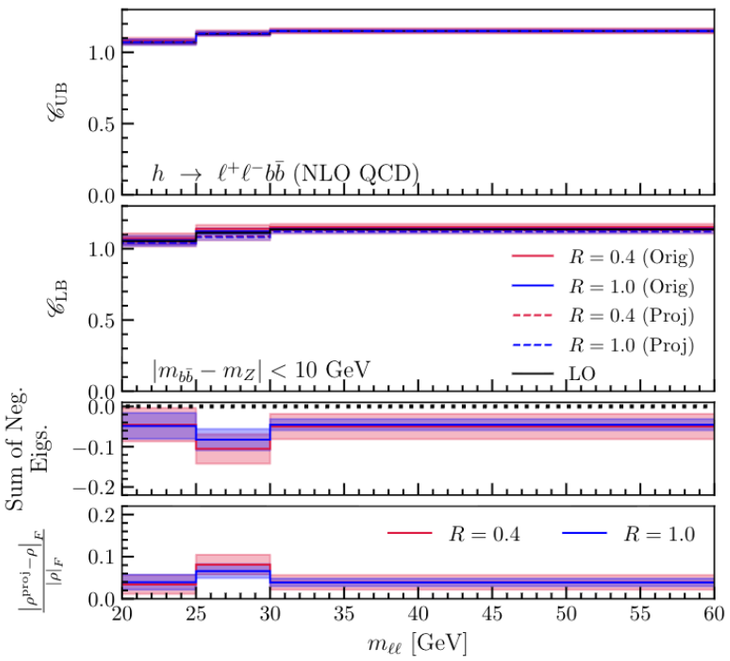

$$\left|\rho^{\text{proj}} - \rho\right|_F \equiv \sqrt{\sum_{i,j} \left|\rho_{ij}^{\text{proj}} - \rho_{ij}\right|^2}.$$

Gonçalves, Kaladharan, **AN** (2026)

$h \to ZZ^* \to \ell^+\ell^- q\bar{q}$ at NLO EW

- For semileptonic decay, still large effects, but smaller than fully leptonic.

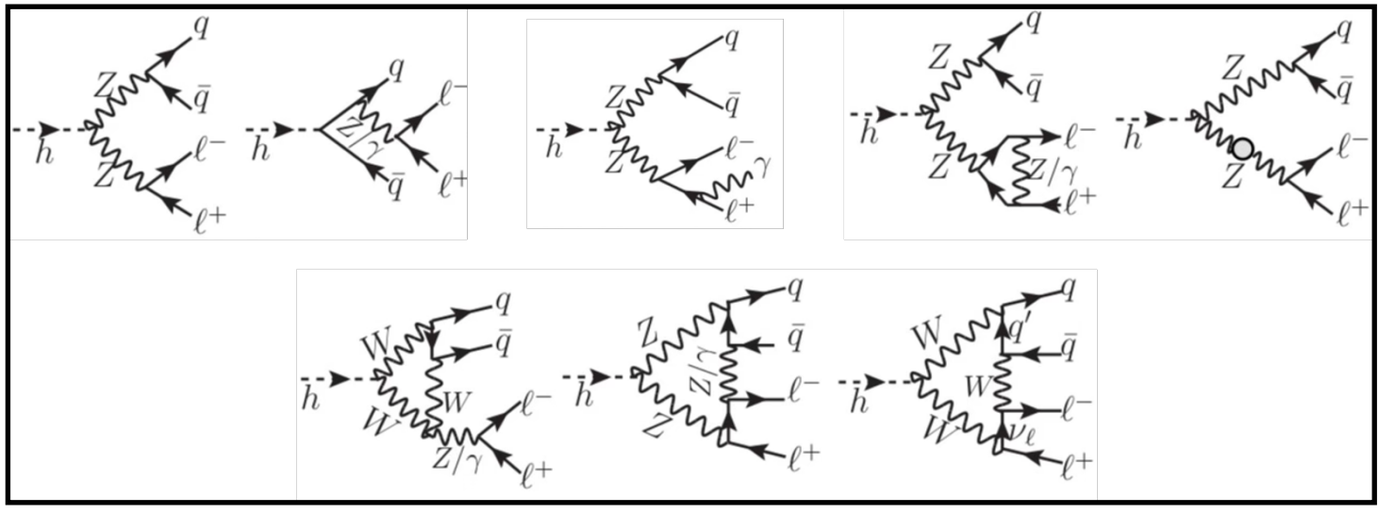

	$h \to \ell^+\ell^- c\bar{c}$		
	LO	$\text{NLO}_{\Delta R<0.1}$	$\text{NLO}_{\Delta R<0.1}/\text{LO}$
$A^1_{2,0}$	$-0.329(1)$	$-0.320(3)$	$0.97(1)$
$A^2_{2,0}$	$-0.328(2)$	$-0.323(2)$	$0.985(9)$
$C_{1,1,1,-1}$	$1.047(4)$	$1.01(1)$	$0.96(1)$
$C_{2,1,2,-1}$	$-1.041(3)$	$-1.043(9)$	$1.002(9)$
$C_{1,0,1,0}$	$-0.766(4)$	$-0.66(8)$	$0.9(1)$
$C_{2,0,2,0}$	$1.233(3)$	$1.23(1)$	$0.997(8)$
$C_{2,2,2,-2}$	$0.764(3)$	$0.758(8)$	$0.99(1)$
	$h \to \ell^+\ell^- b\bar{b}$		
	LO	$\text{NLO}_{\Delta R<0.1}$	$\text{NLO}_{\Delta R<0.1}/\text{LO}$
$A^1_{2,0}$	$-0.329(1)$	$-0.318(4)$	$0.96(1)$
$A^2_{2,0}$	$-0.328(1)$	$-0.323(5)$	$0.98(2)$
$C_{1,1,1,-1}$	$1.046(3)$	$0.945(8)$	$0.903(8)$
$C_{2,1,2,-1}$	$-1.035(3)$	$-1.041(6)$	$1.006(6)$
$C_{1,0,1,0}$	$-0.764(3)$	$-0.60(2)$	$0.79(3)$
$C_{2,0,2,0}$	$1.218(4)$	$1.22(1)$	$1.002(9)$
$C_{2,2,2,-2}$	$0.763(3)$	$0.762(5)$	$0.999(8)$

Gonçalves, Kaladharan, **AN** (2026)

$h \to ZZ^* \to \ell^+\ell^- q\bar{q}$ at NLO EW

- For semileptonic decay, still large effects, but smaller than fully leptonic.
- No sign flip for the L=1 coefficients.

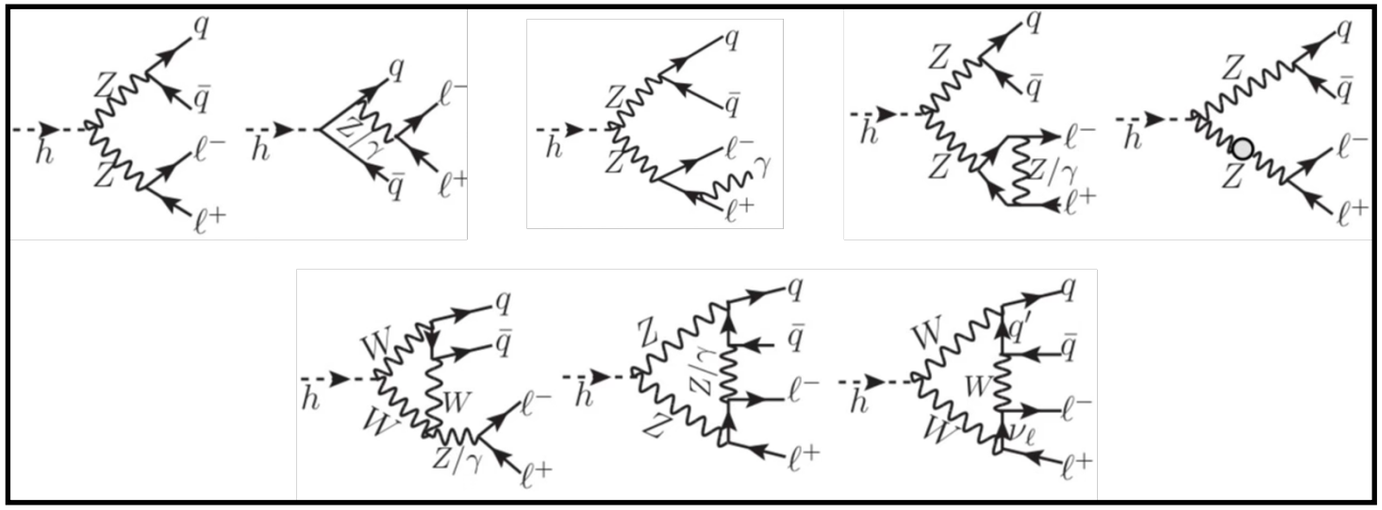

	$h \to \ell^+\ell^- c\bar{c}$		
	LO	$\text{NLO}_{\Delta R<0.1}$	$\text{NLO}_{\Delta R<0.1}/\text{LO}$
$A^1_{2,0}$	$-0.329(1)$	$-0.320(3)$	$0.97(1)$
$A^2_{2,0}$	$-0.328(2)$	$-0.323(2)$	$0.985(9)$
$C_{1,1,1,-1}$	$1.047(4)$	$1.01(1)$	$0.96(1)$
$C_{2,1,2,-1}$	$-1.041(3)$	$-1.043(9)$	$1.002(9)$
$C_{1,0,1,0}$	$-0.766(4)$	$-0.66(8)$	$0.9(1)$
$C_{2,0,2,0}$	$1.233(3)$	$1.23(1)$	$0.997(8)$
$C_{2,2,2,-2}$	$0.764(3)$	$0.758(8)$	$0.99(1)$
	$h \to \ell^+\ell^- b\bar{b}$		
	LO	$\text{NLO}_{\Delta R<0.1}$	$\text{NLO}_{\Delta R<0.1}/\text{LO}$
$A^1_{2,0}$	$-0.329(1)$	$-0.318(4)$	$0.96(1)$
$A^2_{2,0}$	$-0.328(1)$	$-0.323(5)$	$0.98(2)$
$C_{1,1,1,-1}$	$1.046(3)$	$0.945(8)$	$0.903(8)$
$C_{2,1,2,-1}$	$-1.035(3)$	$-1.041(6)$	$1.006(6)$
$C_{1,0,1,0}$	$-0.764(3)$	$-0.60(2)$	$0.79(3)$
$C_{2,0,2,0}$	$1.218(4)$	$1.22(1)$	$1.002(9)$
$C_{2,2,2,-2}$	$0.763(3)$	$0.762(5)$	$0.999(8)$

Gonçalves, Kaladharan, **AN** (2026)

$h \to ZZ^* \to \ell^+\ell^- q\bar{q}$ at NLO EW

- Reconstructed density matrix is not well defined.
- However, semileptonic decay relatively more stable than fully leptonic.

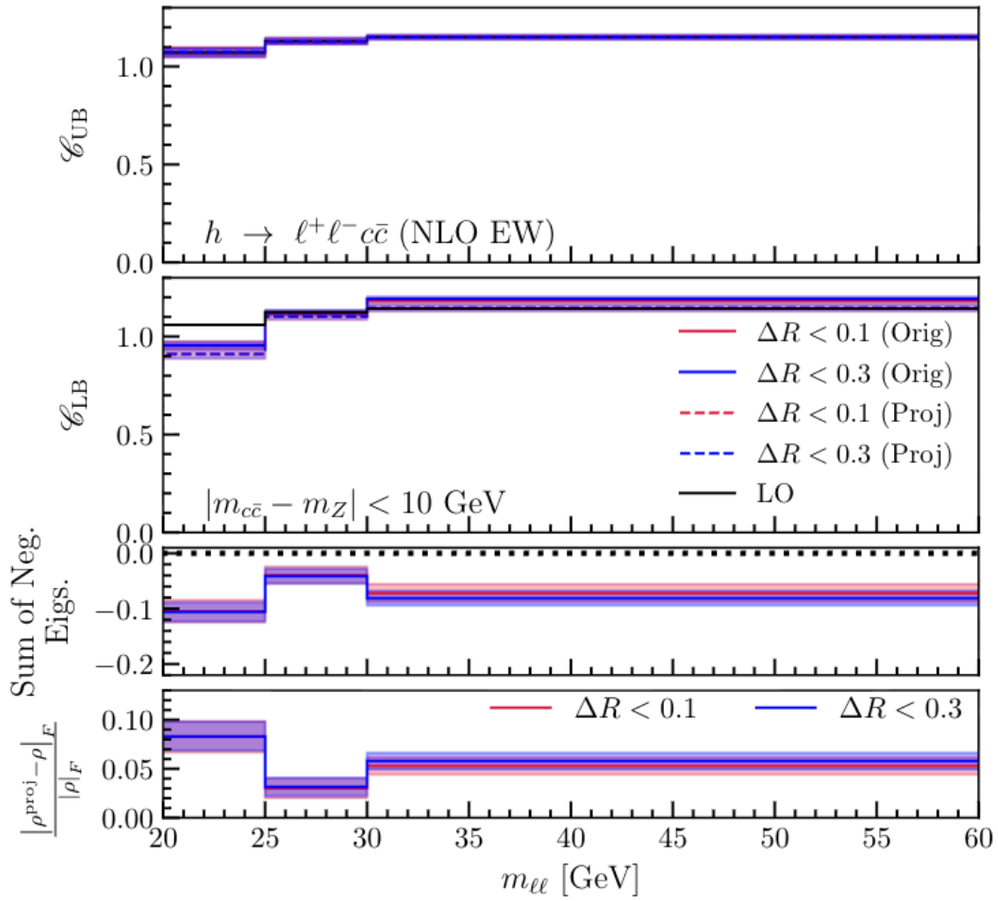

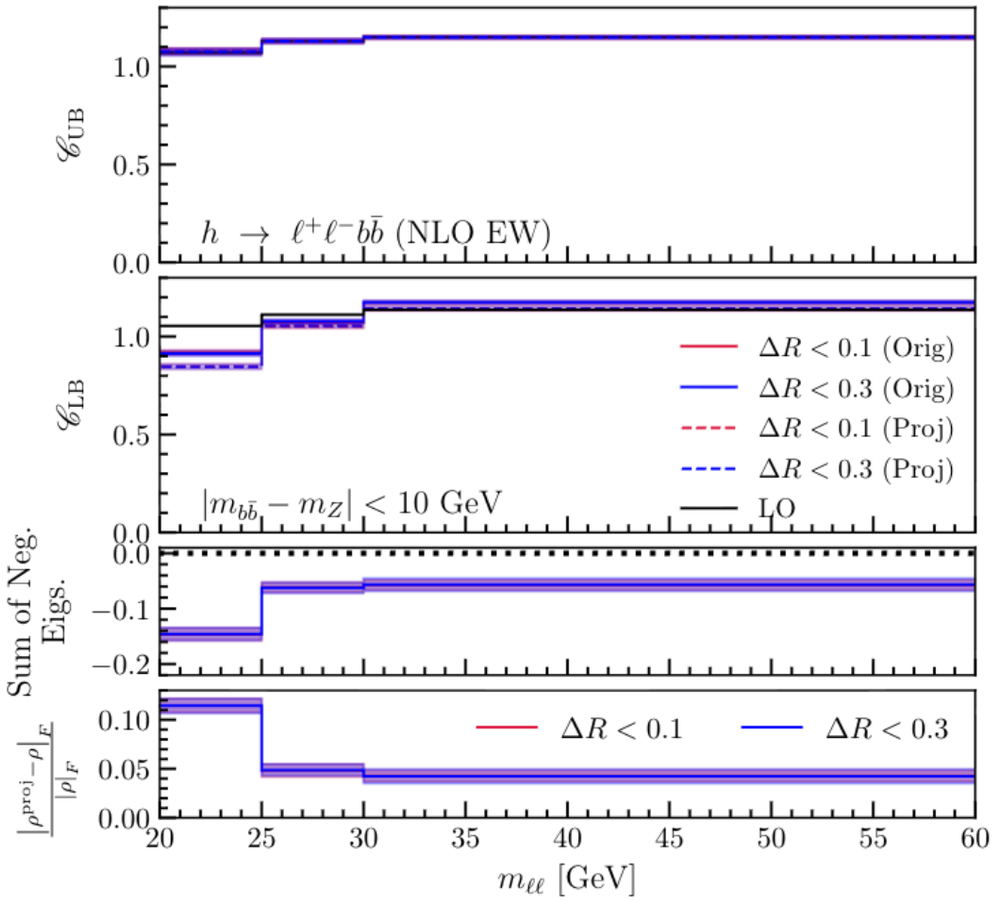

Gonçalves, Kaladharan, **AN** (2026)

$h \to WW^* \to \ell^{\pm}\nu_\ell q\bar{q}'$ at NLO EW

- Affects both sides of the decay.
- New nonzero coefficients.
- Can be suppressed by increasing recombination radius.

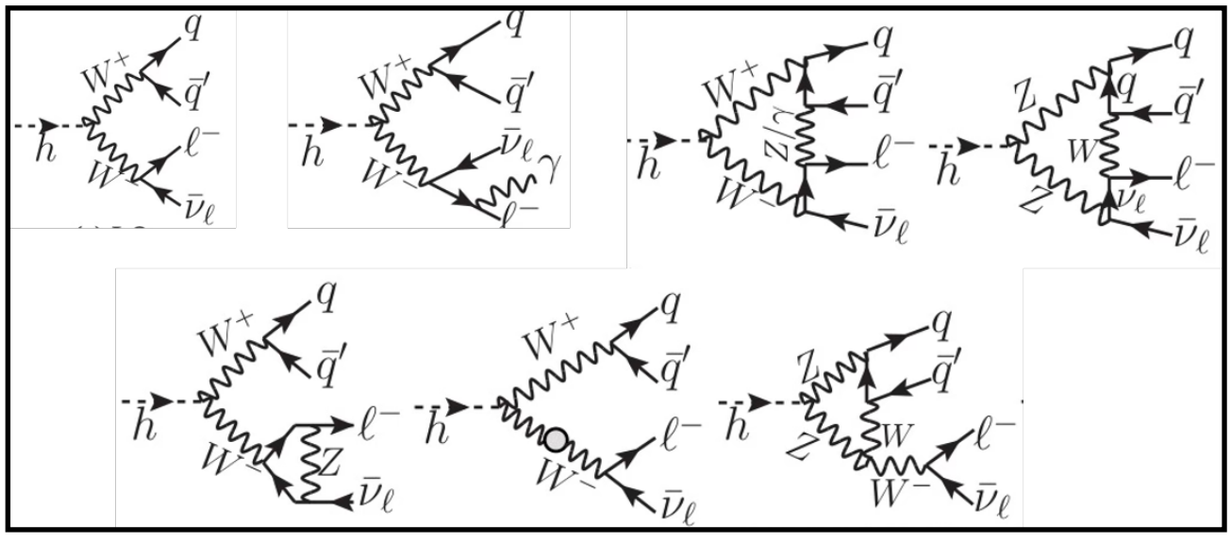

	$h \to \ell^{\pm}\nu_\ell q\bar{q}'$				
Coeff.	LO	$\text{NLO}_{\Delta R<0.1}$	$\text{NLO}_{\Delta R<0.1}/\text{LO}$	$\text{NLO}_{\Delta R<0.3}$	$\text{NLO}_{\Delta R<0.3}/\text{LO}$
$A^1_{2,0}$	$-0.564(1)$	$-0.545(1)$	$0.966(2)$	$-0.548(1)$	$0.972(2)$
$A^2_{2,0}$	$-0.564(1)$	$-0.543(2)$	$0.963(4)$	$-0.547(1)$	$0.970(2)$
$C_{1,1,1,-1}$	$0.9559(6)$	$0.952(2)$	$0.996(2)$	$0.953(2)$	$0.997(2)$
$C_{2,1,2,-1}$	$-0.953(3)$	$-0.956(4)$	$1.003(5)$	$-0.955(3)$	$1.002(4)$
$C_{1,0,1,0}$	$-0.6038(6)$	$-0.611(1)$	$1.012(2)$	$-0.610(1)$	$1.010(2)$
$C_{2,0,2,0}$	$1.401(3)$	$1.382(4)$	$0.986(4)$	$1.384(4)$	$0.988(4)$
$C_{2,2,2,-2}$	$0.604(3)$	$0.601(5)$	$0.99(1)$	$0.602(4)$	$0.997(8)$
$A^1_{1,0}$	0	$-0.0071(8)$	–	$-0.0052(7)$	–
$A^2_{1,0}$	0	$-0.0068(8)$	–	$-0.0050(6)$	–
$C_{2,0,1,0}$	0	$0.013(2)$	–	$0.010(2)$	–
$C_{1,0,2,0}$	0	$0.013(2)$	–	$0.010(2)$	–
$C_{1,-1,2,1}$	0	$-0.008(2)$	–	$-0.005(1)$	–
$C_{2,1,1,-1}$	0	$-0.010(2)$	–	$-0.005(1)$	–

Gonçalves, Kaladharan, **AN** (2026)

$h \to WW^*$ at NLO EW

- Overall smaller effects on the reconstructed density matrix

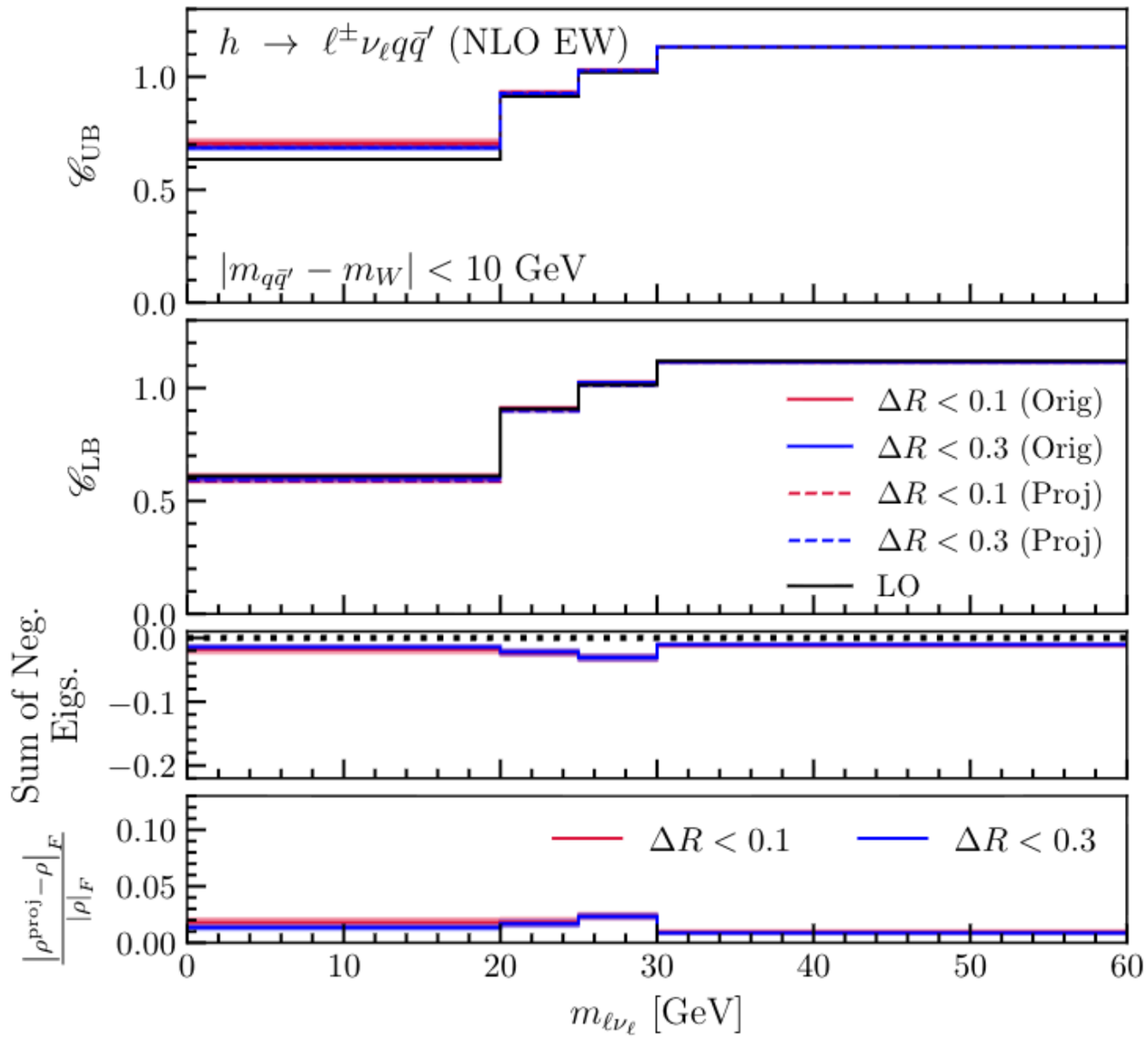

Gonçalves, Kaladharan, **AN** (2026)

Summary

- While higher-order effects induce modest contributions to the Higgs partial decay width, they can induce significant effects in the angular observables.
- Semileptonic h->WW* shows same level of robustness to NLO effects as the leptonic counterpart. In contrast, the effects are smaller for semileptonic h->ZZ* when compared to the leptonic channel.
- Overall, semi-leptonic channels retain an effective two-qutrit description at higher-orders. These findings further motivate the experimental analysis for both semileptonic and leptonic. In particular, for h->WW.

Thanks!

Charge-tagging Effects

- For the $V \to f_1 \bar{f}_2$ decay, the back-to-back kinematics impose $\cos\theta\,,$ $\cos\bar{\theta} = \cos(\pi - \theta) = -\cos\theta$
- Randomly choosing the decay product average over $\cos\theta$ and $-\cos\theta$. This means that the coefficients with odd L vanish. For LO Higgs decay $C_{1,0,1,0} = C_{1,1,1,-1} = C_{1,-1,1,1} = 0$

Coefficient	b	$\bar{b}$	$b/\bar{b}$
$A^1_{2,0}$	$-0.332(9)$	$-0.332(9)$	$-0.332(9)$
$A^2_{2,0}$	$-0.320(9)$	$-0.320(9)$	$-0.320(9)$
$C_{1,0,1,0}$	$-0.73(3)$	$-0.73(3)$	$0.02(3)$
$C_{1,1,1,-1}$	$1.04(2)$	$1.04(2)$	$0.02(2)$
$C_{2,1,2,-1}$	$-1.04(2)$	$-1.04(2)$	$-1.04(2)$
$C_{2,0,2,0}$	$1.25(3)$	$1.25(3)$	$1.25(3)$
$C_{2,2,2,-2}$	$0.73(2)$	$0.73(2)$	$0.73(2)$

- Seven of the eigenvalues of the resulting density matrix are

$$\lambda_{1,2} = \pm\frac{1}{6}C_{212-1}$$

$$\lambda_{3,4} = \pm\frac{1}{6}C_{222-2}$$

- Thus, the resulting density matrix has negative eigenvalues if either

$$C_{2,1,2,-1} \neq 0 \qquad C_{2,2,2,-2} \neq 0$$

- Indeed, for the bb final state we find: $-0.19(1)$, $-0.16(1)$, and $-0.12(1)$ consistent with

$$C_{2,1,2,-1}/6 \approx -0.17 \text{ and } -C_{2,2,2,-2}/6 \approx -0.12$$

- Therefore, charge-tagging is also important for the QT of hadronic final states.

Gonçalves, Kaladharan, **AN** (2026)

More on Mass Effects

- The mapping from f and g to A and C relies on the vanishing of the scalar component of the off-shell propagator.
- If the scalar component does not vanish due to massive final states, the mapping is not exact. Naively using it breaks down the relationship between angular coefficients.
- This can be seen by requiring the hadronic boson to be off-shell at LO

	$h \to \ell^+\nu_\ell \bar{c}s$			$h \to \ell^+\ell^- c\bar{c}$			$h \to \ell^+\ell^- b\bar{b}$		
	$m_c = 0$	$m_c = 1.3$ GeV	Ratio	$m_c = 0$	$m_c = 1.3$ GeV	Ratio	$m_b = 0$	$m_b = 4.5$ GeV	Ratio
$A^1_{2,0}$	$-0.754(3)$	$-0.752(3)$	$0.997(5)$	$-0.408(2)$	$-0.413(2)$	$1.012(7)$	$-0.408(2)$	$-0.435(2)$	$1.066(7)$
$A^2_{2,0}$	$-0.752(3)$	$-0.751(3)$	$0.998(5)$	$-0.408(2)$	$-0.404(2)$	$0.985(7)$	$-0.409(2)$	$-0.380(2)$	$0.929(6)$
$C_{1,0,1,0}$	$-0.472(2)$	$-0.472(2)$	$1.000(5)$	$-0.713(8)$	$-0.720(8)$	$1.01(1)$	$-0.710(7)$	$-0.737(7)$	$0.96(1)$
$C_{1,1,1,-1}$	$0.975(2)$	$0.976(2)$	$1.001(2)$	$1.050(7)$	$1.065(7)$	$1.014(9)$	$1.046(6)$	$1.075(6)$	$1.027(8)$
$C_{2,1,2,-1}$	$-0.982(6)$	$-0.971(6)$	$0.989(8)$	$-1.042(5)$	$-1.043(5)$	$1.001(6)$	$-1.043(5)$	$-0.984(5)$	$0.943(6)$
$C_{2,0,2,0}$	$1.537(8)$	$1.537(8)$	$1.000(7)$	$1.292(7)$	$1.282(7)$	$0.992(7)$	$1.283(7)$	$1.204(7)$	$0.938(7)$
$C_{2,2,2,-2}$	$0.465(8)$	$0.467(8)$	$1.00(2)$	$0.709(6)$	$0.705(6)$	$0.99(1)$	$0.712(6)$	$0.672(6)$	$0.94(1)$

- Effects are more relevant for bb final states, while they remain under control for final states involving c quarks.

Gonçalves, Kaladharan, **AN** (2026)